

## ФАЗОВЫЕ ПРЕВРАЩЕНИЯ

PACS numbers: 61.72.Dd, 64.75.Nx, 88.30.rd

### Hydrogen in Nickel: Hydride or Miscibility Gap?

D. N. Movchan, S. M. Teus, G. S. Mogilny, and V. G. Gavriljuk

*G. V. Kurdyumov Institute for Metal Physics, N.A.S. of Ukraine,  
36 Academician Vernadsky Blvd.,  
UA-03680 Kyiv-142, Ukraine*

Using low temperature X-ray diffraction, the phase transformations in the hydrogen-saturated nickel are studied. At the hydrogen degassing, its content in nickel decreases down to H/M ratio of about 0.65. The further decreasing of hydrogen content leads to the two-phase separation, notably, hydrogen-rich and hydrogen-depleted solid solutions with permanent hydrogen concentrations existing while the hydrogen-rich phase does not disappear. Based on the Gibbs' idea about two types of precipitation reactions and available experimental data, it is concluded that, in fact, the so-called Ni-hydride is a hydrogen-rich solid solution, which appears because of miscibility gap in the Ni–H system. At higher hydrogen contents beyond the crown, hydrogen-rich phase exists in the wide concentration range as a supersaturated hydrogen solid solution in nickel, which is also incorrectly interpreted as Ni-hydride.

За допомогою низькотемпературної Рентгенової дифрактометрії було досліджено фазові перетворення в насищенному воднем нікелі. Було визначено, що при дегазації водню його вміст у нікелі зменшується до співвідношення H/Me, близького до 0,65. Подальше зменшення вмісту водню призводить до поділу на дві фази — збагачений воднем і збіднений воднем тверді розчини, що містять незмінну кількість водню аж до зникнення збагаченої воднем фази. Спираючись на ідею Гіббса щодо двох типів реакцій утворення і наявні експериментальні дані, зроблено висновок, що насправді так званий гідрид нікелю є твердим розчином водню в нікелі, який виникає внаслідок розриву змішуваності в системі Ni–H. При подальшому збільшенні вмісту водню за межами купола він існує в широкому інтервалі концентрацій як перенасичений твердий розчин водню в нікелі, котрий некоректно інтерпретують як гідрид нікелю.

Посредством низкотемпературной рентгеновской дифрактометрии были исследованы фазовые превращения в насыщенном водородом никеле. Было определено, что при дегазации водорода его содержание в никеле

уменьшается до соотношения H/Ме около 0,65. Дальнейшее уменьшение содержания водорода приводит к разделению на две фазы — обогащённый водородом и обеднённый водородом твёрдые растворы, содержащие неизменное количество водорода вплоть до исчезновения обогащённой водородом фазы. Опираясь на идею Гиббса о двух типах реакций выделения и существующие экспериментальные данные, сделан вывод, что в действительности так называемый гидрид никеля является твёрдым раствором водорода в никеле, образующимся в результате разрыва смесимости в системе Ni—H. При дальнейшем увеличении содержания водорода за пределами купола он существует в широком интервале концентраций как пересыщенный твёрдый раствор водорода в никеле, который некорректно интерпретируют как гидрид никеля.

**Key words:** nickel hydride, supersaturated solid solution, miscibility gap, X-ray diffraction.

(Received March 11, 2013; in final version, May 27, 2013)

## 1. INTRODUCTION

The first information about the nickel hydride was published in 1959 [1, 2]. Such interpretation of experimental data was based on a non-diffusional character of hydrogen desorption kinetics. The history of its discovery and stimulating effect of these pioneer works on further studies of metal-hydrogen systems are described in the review [3].

Using X-ray diffraction, the f.c.c. crystal lattice of this new compound with the lattice dilatation of about 6% and H/Ni ratio equal to  $0.6 \pm 0.1$  was determined [4, 5]. Thorough thermodynamic studies of Ni—H systems were performed by Antonov et al. [6, 7] who saturated a pure nickel with hydrogen at different pressures and temperatures and, based on the measurements of electroresistivity, built the  $T-P_{\text{H}_2}$  and  $T-C_{\text{H}}$  phase diagrams for formation and decomposition of Ni-hydride.

Two points are intriguing in these studies: (i) as in the case of Pd—H system [8], the crown exists below 623 K where ‘the low hydrogen  $\gamma_1$ -phase is transformed into  $\gamma_2$ -hydride’ [5, 6]; (ii) like parent nickel, its hydride has the f.c.c. crystal lattice, and the content of hydrogen in this hydride can be increased up to the  $\text{H/M} = 1.0$  and even more [7] within the same crystal lattice.

The aim of this paper is to analyze the Ni-hydride formation based on the X-ray diffraction measurements and Gibbs ideas about two kinds of precipitation reactions in the solid solutions as quoted in [9].

## 2. EXPERIMENTAL

A pure nickel sheet of 0.5 mm in thickness is used for saturation with

hydrogen. The cathodic charging was carried out at room temperature in the aerated 1N H<sub>2</sub>SO<sub>4</sub> solution containing 0.01 g/l NaAsO<sub>2</sub> at the current density of 50 mA/cm<sup>2</sup> for 72 hours. A platinum foil is used as the anode. After charging, the specimens were put into liquid nitrogen to prevent the hydrogen degassing. Specimen installation into the holder of X-ray diffractometer took less than 120 s.

X-ray diffraction (XRD) measurements were carried out in CoK<sub>α</sub>-radiation using Huber diffractometer with one-circle Θ–2Θ goniometer and operating voltage of 30 kV. A computer program controlled the angular movement of both goniometer and counter.

A cryosystem LN-3 produced by Cryo Industries of America Inc. was used for measurements at low temperatures. In contrast to standard cryostats, this system allows the rapid cooling of the sample by the liquid nitrogen flow and measurements at any temperature within the range of +90 to -196°C. The XRD measurements were carried out at -150°C. For hydrogen degassing, the sample in the diffractometer holder was heated to the room temperature (RT) or higher temperatures, held at this temperature for 10 to 15 min and cooled again down to -150°C for further measurements.

The fitting of X-ray diffraction spectra was performed using Peak-Fit program.

### 3. RESULTS

Fragments of the X-ray diffraction patterns after installation of the sample into the holder and subsequent hydrogen degassing are presented in Fig. 1. Two peaks, a small (111)<sub>γ<sub>1</sub></sub> and rather intensive (111)<sub>γ</sub>, are observed just after hydrogen charging and subsequent storage of the sample in liquid nitrogen. The first stage of hydrogen degassing at RT for 10 min leads to the shift of peak (111)<sub>γ</sub> to the position of (111)<sub>γ<sub>2</sub></sub>, whereas peak (111)<sub>γ<sub>1</sub></sub> increases its intensity. Further stages of hydrogen degassing due to holding of the sample at RT and higher temperatures result in the transfer of peaks intensity from γ<sub>2</sub> to γ<sub>1</sub>, which positions are not changed within the error of measurements.

The corresponding lattice parameters are 3.735 Å, 3.718 Å and 3.525 Å for γ, γ<sub>2</sub>, and γ<sub>1</sub>, respectively. Using the data [10] for hydrogen effect on dilatation of metals, one can estimate the atomic ratio H/M as 0.75 ± 0.005 for γ, 0.65 ± 0.005 for γ<sub>2</sub> and 0.02 ± 0.005 for γ<sub>1</sub>. The H/M ratio n<sub>γ<sub>1</sub></sub><sup>max</sup>, as determined in the present study, is consistent with n<sub>γ<sub>1</sub></sub><sup>max</sup> < 0.02 in [11].

After disappearance of γ<sub>2</sub> reflection, the sample was again heated to 90°C for 10 min and finally held for two weeks at RT. The position of peak (111)<sub>γ<sub>1</sub></sub> was actually not changed. It is relevant to note that, within the accuracy of measurements, the γ<sub>1</sub> peak practically cannot be distinguished from that for pure nickel with the lattice parameter of

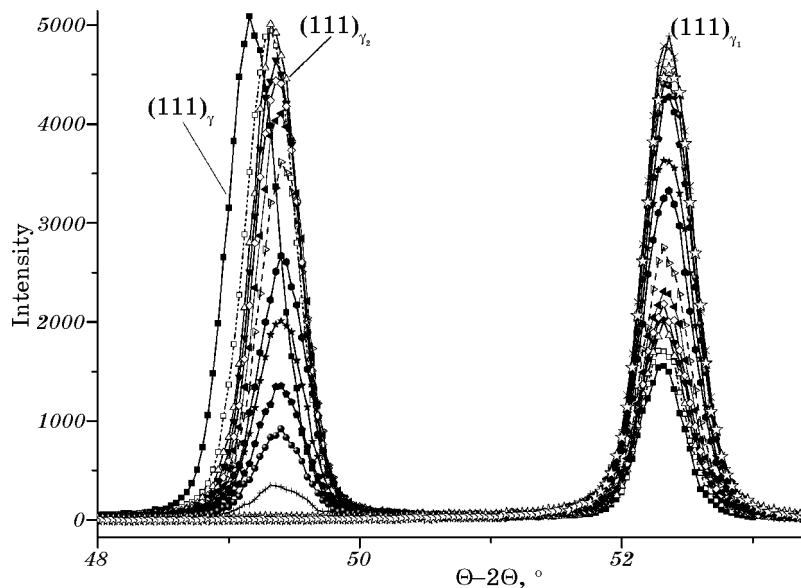


**Fig. 1.** X-ray diffraction for hydrogen-charged nickel. Measurements at  $-155 \pm 5^\circ\text{C}$  with subsequent holding at higher temperatures. Chronological order of measurements: ■—immediately after charging, storage in liquid nitrogen and installation into the diffractometer holder, ···—after holding at  $220^\circ\text{C}$  for 10 minutes, △—after holding at  $220^\circ\text{C}$  for 10 minutes, ▲—after holding at  $190^\circ\text{C}$  for 10 minutes, ◇—after holding at  $190^\circ\text{C}$  for 10 minutes, ▵—after holding at  $190^\circ\text{C}$  for 10 minutes, -·-—after holding at  $460^\circ\text{C}$  for 10 minutes, ●—after holding at  $700^\circ\text{C}$  for 10 minutes, ◆—after holding at  $700^\circ\text{C}$  for 10 minutes, ★—after holding at  $670^\circ\text{C}$  for 15 minutes, ◆—after holding at  $720^\circ\text{C}$  for 15 minutes, +—after holding at  $820^\circ\text{C}$  for 20 minutes, ×—after holding at  $900^\circ\text{C}$  for 44 minutes, ☆—after two weeks holding specimen at RT.

3.5243 Å [12].

#### 4. DISCUSSION

The obtained results should be discussed in terms of two types of precipitation reactions described by the father of thermodynamics J. Willard Gibbs (see, e.g., [9]).

The first reaction occurs if the Gibbs energy  $g$  of a supersaturated  $\gamma$  solid solution cannot be spontaneously reduced to its minimum at a given temperature  $T_1$  because the free energy-composition curve has no maximum and, correspondingly, its curvature  $\partial g^2 / \partial c^2$  is always positive (see Fig. 2, a). In this case, the free energy can be decreased only if some distinctly different new  $\beta$ -phase is nucleated with a lower free energy, so that the total energy of the  $\gamma$ - and  $\beta$ -phases mixture is locat-

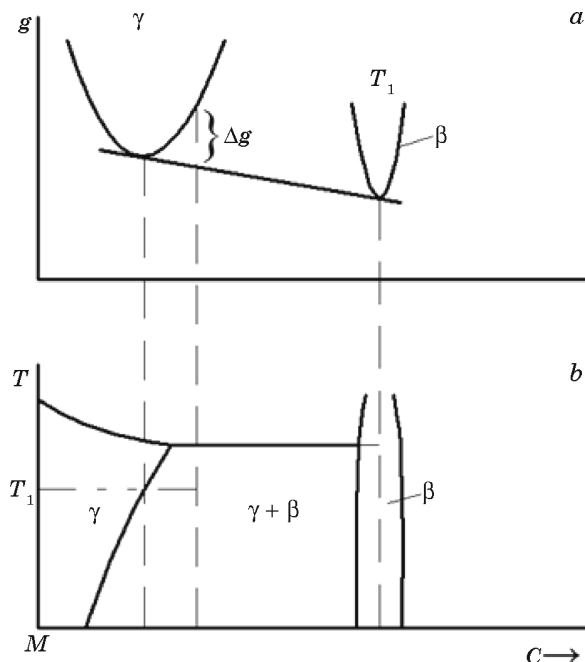


**Fig. 2.** Gibbs energy  $g$  and a corresponding fragment of the phase diagram as functions of chemical compositions and temperature for the case of precipitation of a chemical compound from the supersaturated solid solution (a scheme).

ed at the tangent line connecting their free energy curves and  $\Delta g$  is the energy gain of such a ‘nucleation and growth’ reaction. A corresponding phase diagram is presented in Fig. 2, b.

As an example, one can refer to the precipitation of  $\gamma$ -phase  $\text{Fe}_4\text{N}$  with the f.c.c. crystal lattice from the supersaturated solid solution of nitrogen in the  $\alpha$ -iron having the b.c.c. crystal lattice  $\alpha$  at low temperatures or  $\gamma$  above  $590^\circ\text{C}$  (see, e.g., [13]). A conclusive case is also represented by the precipitated reactions in the solid solution of zinc in copper where, with increasing Zn content, the  $\alpha$ ,  $\beta$ ,  $\gamma$ , and  $\epsilon$  electron compounds are consecutively transformed having, respectively, the f.c.c., b.c.c., complicated cubic and h.c.p. crystal lattices.

The other case occurs if the precipitated phase has the same crystal lattice as the parent one. The free energy of this system is described by a single curve having a maximum and two minima (Fig. 3, a). As a result (see, e.g., [14]), below some critical temperature called as ‘consolute point’, the supersaturated solid solution is decomposed into two phases of fixed compositions (Fig. 3, b). A mechanism of such reaction can be spinodal decomposition or continuous ordering, if the concentration of the supersaturated solid solution is located between two inflections points on the free energy-composition curve (marked with

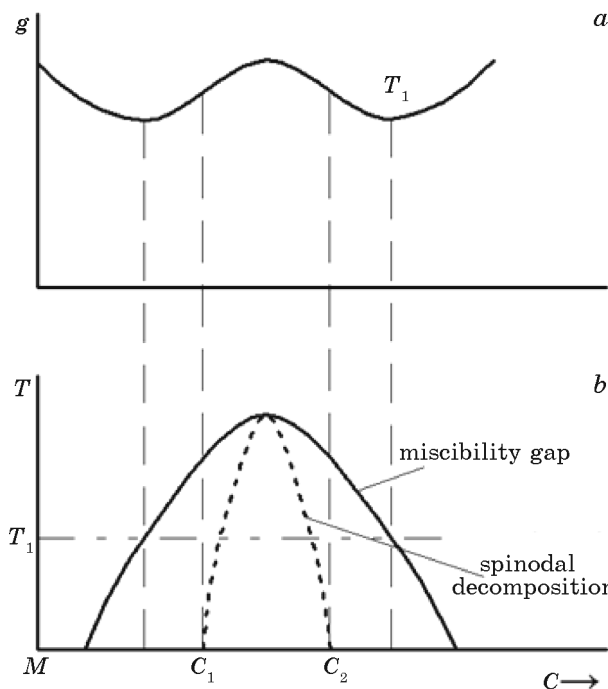


**Fig. 3.** Gibbs energy  $g$  and a corresponding fragment of the phase diagram as functions of chemical compositions and temperature for the case of miscibility gap in the solid solution (a scheme).

dashed lines in Fig. 3, a), where the curvature  $\partial g^2 / \partial c^2$  becomes negative. The corresponding dotted lines in Fig. 3, b do not belong to the phase diagram and just mark the temperature-concentration area where the composition wave with a constant wavelength is formed during spinodal reaction. Beyond this area but between the minima on the free energy curve, correspondingly between the solid and dotted lines of the crown in the phase diagram (Fig. 3, b), the nucleation reaction occurs.

Based on these considerations, let us analyze the obtained experimental data and available published results. In accordance with [4, 5], the peak  $\gamma_2$  corresponds to the same f.c.c. crystal lattice as that of the parent nickel, which suggests the second type of the above mentioned reactions. The two-phase separation  $\gamma_1 - \gamma_2$  and the exchange by their intensities during hydrogen degassing clearly correspond to the miscibility gap.

In the first measurement after sample installation, the peak  $\gamma$  is seen in the diffraction pattern along with a small peak  $\gamma_1$ . It is relevant to note in this relation that, in case of gaseous charging under high hydrogen pressures, a single  $\gamma$  phase is observed for H/M ratio from 0.7

up to 1.25 [7]. Taking this into account, the existence of a small amount of  $\gamma_1$ -phase along with the intensive  $\gamma$ -phase can be related to a not sufficiently homogeneous hydrogen profile.

The main difference between solid solutions and chemical compounds is that first ones exist in a large concentration range, whereas chemical compounds are characterized by the stoichiometric compositions, which deviations are rather small.

Therefore, the shift of peak  $\gamma$  to the position of  $\gamma_2$  due to hydrogen degassing demonstrates the approach of the H-content in a single solid solution to the crown in the Ni-H phase diagram where it is decomposed into  $\gamma_1$  and  $\gamma_2$ . The subsequent exchange by intensities between  $\gamma_2$  and  $\gamma_1$  corresponds to the case when, with decreasing hydrogen content, the mass balance of conjugated phases is controlled by the movement of the figurative point along the conode, whereas the compositions of  $\gamma_2$  and  $\gamma_1$  should remain unchanged.

In fact, such interpretation is consistent with the experimental data in [7] for gaseous hydrogenation (see Fig. 4), where the temperature-pressure area between the homogeneous  $\gamma_1$  and  $\gamma_2$ -phases exists in a

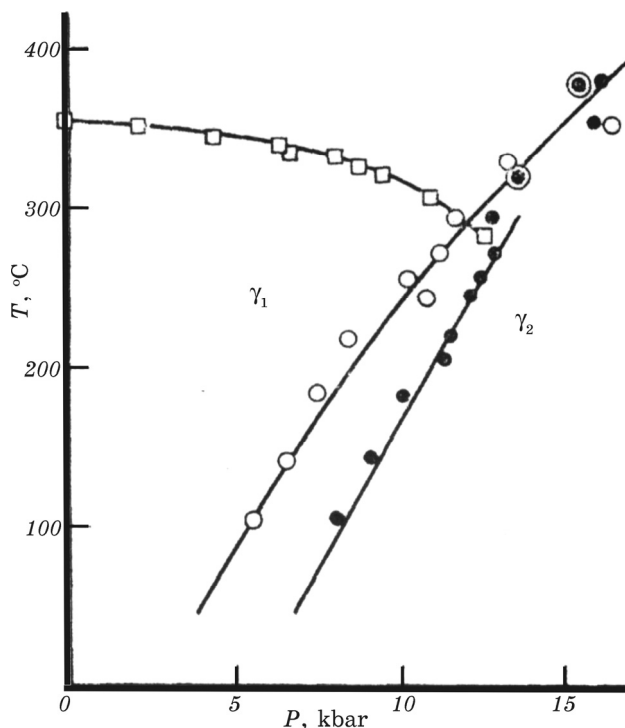


**Fig. 4.** Phase  $T$ - $P$  diagram of Ni-H system according to [7]. Open squares — Curie temperature, closed and open circles — pressures of  $\gamma_1 \rightarrow \gamma_2$ - and  $\gamma_2 \rightarrow \gamma_1$ -transitions, respectively.

broad range of hydrogen pressures, *i.e.* hydrogen contents, at low temperatures and is being confined with increasing temperature. A similar result is also obtained in [15], where, using gaseous high-pressure hydrogenation, the two phase separation occurred with the consolute temperature of about 360°C.

It is relevant to note that an intriguing argument used as apparent confirmation for formation of the nickel as well as other metal hydrides is the sharp decrease of the hydrogen-caused dilatation of the crystal lattice when hydrogen content exceeds the H/M ratio of 0.6 to 0.7 (see, *e.g.*, [3, 16]). It was ascribed to the occupation of tetrahedral interstitial sites by hydrogen atoms, which should decrease the lattice dilatation (*e.g.*, [7]), or to the decrease of the state density at the Fermi level (*e.g.*, [17]). An alternative interpretation can be the hydrogen-caused increase in the thermodynamically equilibrium concentration of vacancies and formation of complexes with the hydrogen atoms which slightly contribute to the lattice dilatation (see also [15] and the pioneer studies [18], where the existence of superabundant vacancies was theoretically predicted for interstitial solid solutions, and [19], where this effect was first time observed for hydrogen).

Taking into account the obtained results and available published data, one can critically estimate a number of publications about high pressure hydrides in different metals (*e.g.*, [19, 20]) where, using neutron and X-ray diffractions, the hydrides are claimed to be formed under high hydrogen pressure in a number of *d*-metals: Cr, Mn, Fe, Co, Ni, Mo, Tc, Rh, Pd, Re. All these discovered hydrides exist in a wide range of hydrogen contents, which does not differ them from the solid solutions. In case of Co, Ni, Rh, Pd, they have the same crystal lattice as the parent metal, which suggests that they are just supersaturated solid solutions. In case of Ni and Pd, the crown, *i.e.*, the miscibility gap in the temperature-concentration phase diagrams is proven. In case of Cr, Mn, Fe and Mo, the hydrogen-induced  $\gamma \rightarrow \epsilon$ -transformation occurs, and, like  $\gamma$ , the  $\epsilon$ -phase exists in the wide concentration range, which is not the case for chemical compounds.

Therefore, in comparison with Ti–H and Zr–H systems, where hydrides have definite stoichiometric chemical compositions and their crystal lattices are different from those of parent metals, there is no convincing arguments to denote the above mentioned solid solutions as hydrides.

## 5. SUMMARY

The obtained data of the X-ray diffraction studies and the analysis of available experimental data allow concluding that so-called Ni-hydride results from the separation of the H solid solution into the hydrogen-rich and hydrogen-depleted phases. At higher hydrogen contents be-

yond the crown in the Ni–H phase diagram, a single supersaturated f.c.c. solid solution exists in a wide concentration range without any common signs of hydride formation.

## REFERENCES

1. B. Baranowski and M. Smialowski, *J. Phys. Chem. Solids*, **12**: 206 (1959).
2. B. Baranowski, *Bull. Acad. Polon. Sci.*, **7**: 907 (1959).
3. B. Baranowski and S. M. Filipek, *J. Alloys Compd.*, **404–406**: 2 (2005).
4. A. Yanko, *Bull. Acad. Polon. Sci.*, **8**: 131 (1960).
5. J. W. Cable, E. O. Wollan, and W. C. Koehler, *J. de Physique*, **25**: 460 (1964).
6. Ye. G. Ponyatovsky, V. Ye. Antonov, and I. T. Belash, *Reports of USSR Academy of Sciences*, **229**: 391 (1976) (in Russian).
7. V. E. Antonov, I. T. Belash, and Ye. G. Ponyatovsky, *Reports of USSR Academy of Sciences*, **233**: 1114 (1977) (in Russian).
8. A. J. Maeland and T. R. P. Gibb, *J. Phys. Chem.*, **165**: 1270 (1961).
9. R. D. Doherty, *Physical Metallurgy* (Eds. R. W. Cahn and P. Haasen) (Amsterdam: Elsevier Science BV: 1996), p. 1365.
10. B. Baranowski, S. Majchrzak, and T. B. Flanagan, *J. Phys. F.: Metal Physics*, **1**: 258 (1971).
11. V. G. Tyssen, V. E. Antonov, I. T. Belash, B. K. Ponomarev, and Ye. G. Ponyatovsky, *Reports of USSR Academy of Sciences*, **242**: 1390 (1978) (in Russian).
12. *Tesaurus Fiziki Tvyordogo Tela* (Thesaurus of Solid State Physics) (Ed. V. G. Baryakhtar) (Kiev: Naukova Dumka: 1996) (in Russian), vol. 1, p. 608.
13. M. Hansen and K. Anderko, *Constitution of Binary Alloys* (New York–Toronto–London: McGraw-Hill Inc: 1958), p. 670.
14. A. D. Pelton, *Physical Metallurgy* (Eds. R. W. Cahn and P. Haasen) (Amsterdam: Elsevier Science BV: 1996), p. 478.
15. Y. Shizuku, S. Yamamoto, and Y. Fukai, *J. Alloys Compd.*, **336**: 159 (2002).
16. K. Farrell and M. B. Lewis, *Scr. Metall.*, **15**: 661 (1981).
17. V. A. Somenkov, V. P. Glazkov, A. I. Irodova, and S. Sh. Shilstein, *J. Less-Common Metals*, **129**: 171 (1987).
18. A. A. Smirnov, *Metallofizika*, **12**: 52 (1991) (in Russian).
19. Y. Fukai and N. Okuma, *Jpn. J. Appl. Phys.*, **32**: 1256 (1993).
20. V. E. Antonov, *J. Alloys Compd.*, **330–332**: 110 (2002).